Application of rice husk as an adsorbent for the simultaneous removal of a multicomponent system of dyes: evaluation of the equilibrium and kinetics of the process

Fredy Amaringo[a],*, Angelina Hormaza[b]

[a]*Research Group in Management and Environmental Modeling, GAIA, Universidad de Antioquia, Medellin, Colombia,
email: fredy.amaringo@udea.edu.co*
[b]*Research Group on Synthesis, Reactivity and Transformation of Organic Compounds, "SIRYTCOR," School of Chemistry,
Faculty of Science, Universidad Nacional de Colombia, Sede Medellín, Colombia, email: ahormaza@unal.edu.co*

ABSTRACT

This work shows the adsorption study of a dye mixture onto rice husk (RH) by means of the first-order derivative spectroscopy under a batch system, for which the anionic dye Red 40 (R40) and vat dye Indigo Blue (IB) were selected. This work shows for the first time the use of RH for the adsorption of a dye mixture formed by R40 and vat dye IB. The first-order derivative spectroscopy and analysis under a batch system were implemented. In order to establish the best conditions for the removal of these pollutants, a 2^3 full factorial design was initially carried out for each individual dye and then a 2^4 full factorial design for their mixture. Likewise, the equilibrium of the process was evaluated, taking into account the dyes as both mono-component systems and as part of the binary mixture, finding that Langmuir isotherm model is the one that offers the best fit for the experimental data of R40 ($R^2 = 0.987$) and IB ($R^2 = 0.989$), while competitive Langmuir model is the most suitable for the multicomponent system. As for the kinetics, the pseudo-second-order model shows the best fit for R40 ($R^2 = 0.970$) and IB ($R^2 = 0.989$), evaluated as individual dyes. This pseudo-second-order model also reproduces the experimental data of the mixture adequately. These findings point out that the adsorption of R40-IB dye mixture takes place through a competitive process, which is more favorable for the anionic dye R40. Furthermore, the achieved removal of 64.1% for this multicomponent system of dyes confirms that RH provides a potential adsorbent capacity and that this methodology is a viable approach for the treatment of colored effluents.

Keywords: Adsorption; Binary mixture; Isotherms; Kinetic models; Indigo Blue; Agricultural by-product

1. Introduction

Developing countries face a serious problem of water resources contamination due to the lack of investment in wastewater treatment systems. These pollutants are generally incorporated into surface water through the discharge of effluents from a variety of processes of petrochemical, food, chemical, and textile industries [1]. In the case of the textile industry, discharges include organic salts, fixatives, starch, peroxides, surfactants, and a considerable percentage of the dye used for staining, making it difficult to treat this type of colored effluents [2,3]. This fact is aggravated by the chemical stability of the dyes, whose resistance to factors such as light and temperature has cataloged them as recalcitrant. In addition, these dissolved dyes generate alkaline waters with high values of biological oxygen demand and chemical oxygen demand, leading to anoxic conditions that seriously affect organisms at different trophic levels [4,5]. Particularly, blue indigo vat dye is widely used in the textile industry and is characterized as a granular or dark blue powder, it has

* Corresponding author.

an estimated annual production of 13,000 tons and is used especially for blue-jeans staining [6].

For industrial-level dyeing process, water-insoluble IB must be reduced with stoichiometric amounts of sodium dithionite, using a relation of 4:1 with respect to the dye, becoming its leuco form, characterized by its yellow color and water solubility. In this way, sulfates, sulfites, and thiosulfate ions result as by-products, which have harmful effects on the environment as well as a corrosive effect on wastewater pipes [7]. Conversely, red 40 (R40) dye is soluble in water and is used mainly in the food industry for the production of meat products, candies, and pastry. However, it has been reported that azo dyes can trigger intolerance in those people affected by salicylates. R40 is a histamine releaser and can intensify the symptoms of asthma [8,9]. Likewise, it is involved in hyperactivity in children, when used in combination with benzoates [10]. Moreover, it is important to highlight that the dyeing process is not totally efficient, so textile and food industries discharge effluents with high contents of them, so that in the case of IB, it is estimated that a percentage of 8%–20% is released in water bodies [11] and for azo dyes such as R40 from 10% to 15% [12].

Among the methodologies for dissolved dyes treatment, adsorption has shown to be one of the most efficient as a reason of the nonfragmentation of the molecule, high efficiency and reuse of the adsorbent; overcoming disadvantages of traditional methods such as photochemical which gives rise to color disappearance but generates much more toxic compounds, as for instance aromatic amines [13]. Besides, flocculation, economically available, allows a rapid purification of colored effluents by a simple procedure and with a satisfactory efficiency, however, the generation of sludge derived from the addition of emulsifiers and reagents is a difficult problem to solve [14]. For its part, activated carbon is a good adsorbent of both dyes and metals because of its large surface area; this material was used classically in removal processes. Nevertheless, its high cost and restricted polarity limit its use [15–18]. These drawbacks have encouraged the search for nonconventional, efficient, and cheap adsorbents. In this sense, agricultural by-products have shown to be highly efficient in the removal of colored effluents. A wide variety of them have been evaluated, for example, rice husk (RH), sugarcane bagasse, corn cob, pine sawdust, and flower wastes [19–21]. In addition, these residues are abundant and have a low-cost, translating it into a substantial economic reduction for this process. Thus, the use of this waste would enable a sustainable and environmentally friendly treatment [22].

It should be noted that most research concerning to dye removal has been focused on the evaluation of this pollutants, considering them as mono-systems [21–23]. However, the reality of companies that use dyes in their processes corresponds to a very different situation, since they released effluents containing a mixture of two or more compounds. The presence of that mixture implies an analytical complexity in the quantification of each dye due to the overlapping of their bands. This fact explains in part the few information available on adsorption about multicomponent systems [24,25]. Derivative spectrophotometry is a suitable, economical, fast, and accurate technique for dye mixtures analysis, since it allows the separation of overlapped signals, reducing the effect of spectral interferences caused by the presence of other compounds in a sample [26]. One of the most recent works is reported by Asfaram et al. who recorded the simultaneous removal of malachite green and violet crystal dyes on *Yarrowia lipolytica* trough derivative spectroscopy, achieving an adsorption of 99.9% and 96.5%, respectively [27]. Despite its high efficiency, scaling up this process is not feasible due to the large amount of yeast required to start it.

Rice is one of the major crops in Colombia, surpassed only by coffee and corn [28], with an annual production reaching 2.5 million tons of paddy rice and 1.7 million tons of white rice, with an estimated amount of RH close to 400,000 tons that are usually discarded [29]. With these precedents and seeking a more realistic approach to the problem of dye-bearing effluents, this research evaluated for the first time the absorption capacity of the RH, as a nonconventional and low-cost adsorbent material, in the removal of the binary mixture IB-R40 under batch system. The first-order derivative spectroscopy was implemented to quantify the dye mixture. The adsorption was optimized through a 2^4 full factorial design which included the factors: pH, temperature, agitation speed, concentration of a single dye, and of the binary mixture of dyes. In addition to this, Langmuir and Freundlich isotherm models, as well as the kinetic models of pseudo-first-order and pseudo-second-order, were analyzed for individual dyes, as well as for their mixture to have insights about the adsorption process that occurs between the IB-R40 dyes onto RH.

2. Materials and methods

2.1. Adsorbent preparation

Natural RH was obtained from rice agroindustries located in the department of Córdoba, Colombia. It is worth mentioning that sampling was carried out at random in five collection points during the first quarter of the year to avoid humidity present in the open storage sites. Its pretreatment included three washes with distilled water, drying at a temperature of 80°C during 24 h in an A&E HDF-64 digital oven, grinding, and sieving in order to obtain particles with a size between 0.3 and 0.5 mm.

2.2. Preparation of the dye solution

Standard solutions of R40 and IB dyes, whose chemical structures are presented in Figs. 1(a) and (b), and their respective mixture was prepared in deionized water at a concentration of 100 mg/L for IB and 30 mg/L for R40, from which corresponding dilutions were made for each dye calibration curve. These compounds were measured at their maximum absorbance wavelength, that is, λ_{max} = 505 and 708 nm for R40 and IB, respectively. For the calibration curve of the binary mixture, equal volumes of individual dye solutions were taken, and wavelengths of maximum absorbance were determined by first-order derivative spectroscopy.

2.3. Adsorption of R40 and IB under batch system

Adsorption studies were carried out under a batch system, for which a shaker with an incubator was used to maintain a constant temperature and agitation. All tests
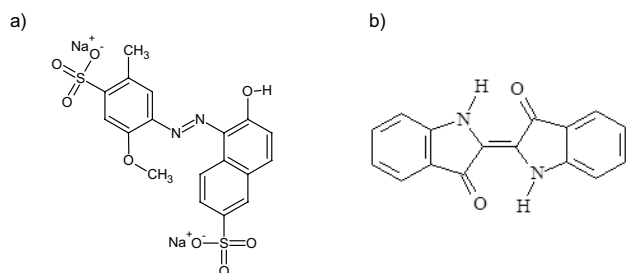
Fig. 1. (a) Chemical structure of R40. (b) Chemical structure of IB.

were made in triplicate for statistical support. The quantification of R40 and IB, both individually and in mixture, was performed by UV-vis spectrophotometry using a Perkin–Elmer double beam lambda 35 spectrophotometer. In order to achieve an efficient removal of both individual dyes, R40 and IB, and their respective mixture, a statistical design of experiments were implemented.

The adsorption percentage of individual dyes onto RH was determined by the Eq. (1) as follows:

$$\text{adsorption}\% = \frac{C_o - C_e}{C_o} \times 100\% \tag{1}$$

where C_o is the initial concentration of dye and C_e is the equilibrium concentration of dye.

2.4. Factorial design: removal of the dyes as an individual system and as part of the binary mixture

For the removal of the individual dyes, a 2^3 full factorial design was carried out with 8 experiments and 3 repetitions for a total of 24 experimental units with level values (+1) and (−1). The selected factors were the adsorbent dosage, initial dye concentration, and contact time at room temperature; pH = 2.0, particle size between 0.3–0.5 mm, and stirring speed of 180 rpm.

For the mixture removal, a complete 2^4 full factorial design was performed with 16 experiments and 3 replicates for a total of 48 experimental units with level values (+1) and (−1), the 4 evaluated factors were adsorbent dosage, contact time, and the initial concentrations of each dye. For results analysis, the software Statgraphics Centurion XV free version was used.

2.5. Equilibrium the of dyes as a mono-system and as part of the multicomponent system

In order to evaluate the equilibrium of the dyes as mono-component systems, mathematical models were used to calculate the amount of dye adhered to the adsorbent, starting from a known initial concentration of the dye and its concentration in equilibrium. In particular, Langmuir and Freundlich models were implemented.

2.5.1. Langmuir model

Langmuir isotherm model considers that adsorption takes place exclusively at specific sites located on the adsorbent surface, only one molecule of the adsorbate is adsorbed or bounded to each site, there is no interaction between

adjacent retained molecules and the heat of adsorption is the same for all sites. This model is represented mathematically by Eq. (2) as follows [30]:

$$q_e = q_{max} \frac{bC_e}{1 + bC_e} \tag{2}$$

where q_{max} is the maximum capacity of adsorption of the dye under given conditions, in this case the dye (mg/g), b is the Langmuir constant indicating the affinity of the adsorbate for the adsorbent, q_e is the amount of adsorbate transferred to the surface of the adsorbent, and C_e is the concentration of the adsorbate in equilibrium.

2.5.2. Freundlich model

Freundlich equation is another model widely used in liquid-solid systems. It assumes that the surface of the adsorbent is heterogeneous and adsorption positions have different affinities, occupying first those of greater affinity and then the others [31]. This model is described mathematically by Eq. (3) as follows:

$$q_e = K_F C_e^{1/n} \tag{3}$$

where K_F is the Freundlich constant related to the adsorption capacity of the dye, n is the Freundlich constant associated to the intensity of the adsorption, q_e is the amount of adsorbate transferred to the surface of the adsorbent, and C_e is the concentration of the adsorbate in the equilibrium.

2.5.3. Multicomponent isotherm models

When having a mixture of two or more adsorbates, compounds may experience three situations: an increase in the adsorption, an independent behavior, or an interference with each other. In these cases, the final equilibrium positions are governed by competitive interactions, described through mathematical models [32]. In this work, the equilibrium study of the dye mixture was carried out through three mathematical models: competitive extended Langmuir, modified extended Langmuir, and multicomponent Freundlich [33].

2.5.3.1. Competitive extended Langmuir model

This model assumes that the competition among different components depends on the relationship among the concentration of adsorbates, therefore it is applied to predict the adsorption behavior of a material in a multicomponent system using the parameters of individual components [34]. The competitive extended Langmuir model is represented by Eq. (4) as follows:

$$q_{e,i} = \frac{q_{max,i} K_i C_{eq,i}}{1 + \sum_{j=1}^{n} K_j C_{eq,j}} \tag{4}$$

where $q_{max,i}$ is the maximum adsorption capacity of "i" adsorbate in the one-component system, K_i and K_j are Langmuir constants that indicate the affinity for active sites, $C_{eq,i}$ and $C_{eq,j}$ are the concentrations in "i" and "j" adsorbates the equilibrium, and $q_{e,i}$ is the amount of "i" adsorbate which has
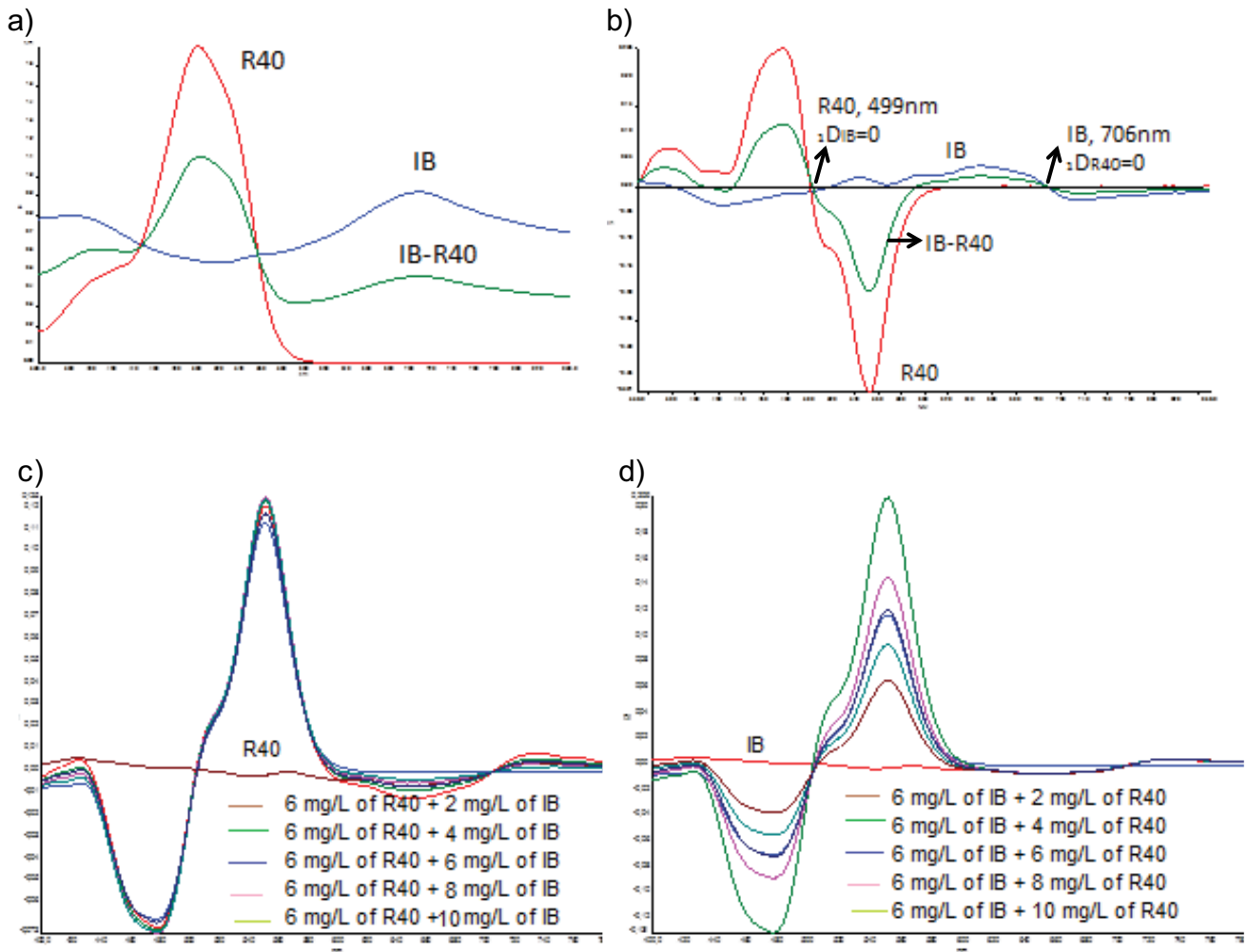
Fig. 2. Spectroscopic study of the IB-R40 dye mixture, (a) IB, R40 and mixture of IB-R40 spectrum (initial concentration 30 mg/L), (b) First-order derivative spectrum of IB and R40 individual solutions and their binary mixture (initial concentration 30 mg/L), (c) First-order derivative spectrum of the IB-R40 mixture, keeping the concentration of R40 (6 mg/L) constant and the concentration of IB (2–10 mg/L), and (d) First-order derivative spectrum of the IB-R40 mixture, keeping the concentration of IB constant (6 mg/L) and the concentration of R40 (2–10 mg/L).

been transferred to the surface of the adsorbent in the multi-component system.

2.5.3.2. Modified extended Langmuir model

When there is a mixture of dyes, adsorption constants of the individual isotherms could not describe the interactions between adsorbates. The addition of η correction parameters to the classical Langmuir competitive equation represents the complexity of the process, so it is necessary to use the modified extended Langmuir equation, represented in Eq. (5) as follows [35]:

$$q_{e,i} = \frac{q_{\max,i} K_{a,i} \left(C_{eq,i} / \eta_i \right)}{1 + \sum_{j=1}^{n} K_{a,j} \left(C_{eq,j} / \eta_j \right)} \quad (5)$$

where $q_{\max,i}$ is the Langmuir constant of the extended model which denotes the maximum adsorption capacity of each "i" adsorbate in the mono-component system, $K_{a,i}$ and $K_{a,j}$ are the Langmuir constants that indicate the affinity with the active sites and with "i" and "j" adsorbates heat of adsorption in the mono-component system, $C_{eq,i}$ and $C_{eq,j}$ are the concentration in the equilibrium of "i" and "j" adsorbates, $q_{e,i}$ is the amount of the "i" adsorbate that has been transferred to the surface of the adsorbent in the multicomponent system, and η_i and η_j are the interaction factors of "i" and "j" adsorbates which depend on the other adsorbate.

2.5.3.3. Multicomponent Freundlich model

As previously mentioned, when dealing with a binary mixture of dyes, there is the probability of an interaction between compounds, which can be evaluated through the

Freundlich multicomponent model, represented by Eq. (6) as follows [33]:

$$q_i = K_i C_i \left(\sum_{j=1}^{k} a_{ij} C_j \right)^{m_i - 1}$$ (6)

For a binary system, the following should be taken into account in isotherms:

$$\frac{C_1}{C_2} = \frac{1}{C_2} \beta_1 - a_{12}$$ (7)

$$\frac{C_2}{C_1} = \frac{1}{C_2} \beta_2 - a_{21}$$ (8)

where $\beta_i = \left(\dfrac{q_i}{K_i C_i} \right)^{\frac{1}{m_i} - 1}$ and a_{ij} is the coefficient of competition with $a_{ij} = 1/a_{ji}$, K_i and m_i: are Freundlich constants coming from the mono-component systems with, $m_i = 1/n_i$, q_i and C_i are the amount of "i" adsorbate that has been transferred to the surface of the adsorbent and concentration of "i" solute in the balance, respectively.

The concentration in the dye mixture was calculated by Eqs. (9) and (10), which consider the interaction of the two components A and B [36].

$$C_A = \frac{k_{B2} A_1 - k_{B1} A_2}{k_{A1} k_{B2} - k_{A2} k_{B1}}$$ (9)

$$C_B = \frac{k_{A1} A_2 - k_{A2} A_1}{k_{A1} k_{B2} - k_{A2} k_{B1}}$$ (10)

where C_A, A_1, C_B, and A_2 are the initial concentrations and absorbance of R40 and IB in the mixture, respectively. While k_{A1}, k_{A2}, k_{B1}, and k_{B2} are the constants of R40 and IB in the calibration curve in the mixture at their maximum absorbance wavelength, respectively.

For equilibrium evaluation of the mixture, stock solutions of 100 mg/L for IB and 30 mg/L for R40 were prepared in Erlenmeyer flasks of 100 mL at pH = 2.0. For IB, nine solutions from 10 to 90 mg/L were prepared, increasing the concentration in 10 mg/L in each solution. For R40, nine solutions from 3.0 to 27 mg/L were also prepared, increasing the concentration in 3.0 mg/L in each solution.

For the competitive adsorption isotherms, 10 mL of each solution of IB and R40 were taken for a total volume of 20 mL of mixture, 120 mg of RH were added with a particle size between 0.3 and 0.5 mm. Erlenmeyer flasks were sealed and placed on a shaker with incubator for keeping the temperature constant during 24 h at a stirring speed of 180 rpm. Preliminary tests showed that a contact time of 24 h was enough to reach equilibrium. To determine the residual dye, 2.0 mL of sample containing IB and R40 were taken to be measured in the UV-vis spectrophotometer at wavelengths λ_{max} = 706 nm for IB and λ_{max} = 499 nm for R40 in the mixture. All analyses were performed in triplicate.

2.5.4. Kinetics of the dyes as a mono-system and as part of the multicomponent system

To assess the kinetics of the dyes as mono-component systems, two models were used, pseudo-first order and pseudo-second order.

2.5.4.1. Pseudo first order equation

It is one of the most widely used kinetic models that can be expressed by Eq. (11) as follows [37]:

$$\log \left(\frac{q_e}{q_e - q_t} \right) = \frac{k_1 t}{2.303}$$ (11)

where q_e and q_t are the amount of adsorbate transferred to the surface of the adsorbent at equilibrium and time t, respectively, is the speed constant in min^{-1}. By plotting, $\log \left(\dfrac{q_e}{q_e - q_t} \right)$ versus t, the speed constant k_1 from the slope can be calculated.

2.5.4.2. Pseudo-second-order equation

It is one of the most observed models in adsorption processes. It is based on the adsorption capacity in equilibrium and assumes that the adsorption speed is directly proportional to the square of available sites, it is expressed mathematically through Eq. (12) as follows [38,39]:

$$\frac{t}{q_t} = \frac{1}{k_2' q_e^2} + \frac{1}{q_e} t$$ (12)

where q_t is the amount of dye adsorbed on the surface of the adsorbent overtime (mg/g), t is the time in (min), q_e is the amount of adsorbate on the surface of the adsorbent at equilibrium (mg/g), and k_2' speed constant (g/mg min). By plotting, t/q_t versus t, the value of the constant k_2' from the intercept can be obtained.

2.5.4.3. Evaluation of the kinetics of the process

Solutions were prepared from the best conditions of the statistical design, that is, 30 mg/L of IB and 10 mg/L of R40. These concentrations were taken as fixed and the kinetics of the process was evaluated at several temperatures.

For this, 20 mL of each solution were taken in Erlenmeyer flasks of 100 mL, to which 120 mg of RH with particle size between 0.3 and 0.5 mm were added. Erlenmeyer flasks were sealed and placed in a shaker with incubator in order to maintain a constant temperature during the process at a stirring speed of 180 rpm. For R40 the solutions were evaluated during 24 h, changing the sampling time in 15, 30, 60, 120, 180, 360, and 1,440 min; and during 6 h for IB changing the sampling in 5, 15, 30, 60, 120, 180, and 360 min. These samples were measured at the maximum absorption wavelengths of each dye to determine the residual concentration. All analyses were performed in triplicate at temperatures

of 298, 308, 318, and 328 K. Experimental data were correlated with Eqs. (11) and (12) to establish the model that fits the best.

For kinetics evaluation of the mixture, a similar procedure was followed; 10 mL of IB and R40 solution were taken, obtaining final concentrations of 30 mg/L of IB and 10 mg/L of R40, for a total volume of 20 mL of mixture. These concentrations were taken as fixed and were subjected to different temperatures to evaluate their influence on kinetics. The process was evaluated throughout 24 h, fluctuating the sampling time in 15, 30, 60, 120, 180, 360, and 1,440 min. Then, Eqs. (11) and (12) models were applied respectively to establish the best fit.

3. Results and discussion

3.1. First-order derivative spectroscopy

For the simultaneous analysis of the binary mixture of IB and R40 dyes, each with a concentration of 30 mg/L, Fig. 2(a) shows a partial overlap of their maximum absorption bands with respect to the wavelengths of dyes measured individually. This fact indicates the existence of interference between IB and R40 dyes when they are mixed, so the concentrations of these pollutants in the mixture cannot be determined by direct spectroscopy. This analytical drawback was solved by applying first-order derivative spectroscopy, a methodology that allowed the simultaneous determination of each dye quantity in the mixture [24–25]. In Fig. 2(b), it can be seen how the absorption spectrum of first-order derived from IB and R40 changes in individual solutions and in the mixture. This first-order derivative spectrum shows that the concentration of R40 in the mixture was determined at $\lambda = 499$ nm (^{1}D499) in the presence of IB, in which IB absorbance is zero. For IB, the concentration was determined at $\lambda = 706$ nm (^{1}D706) in the presence of R40, when R40 absorbance is zero.

3.1.1. Recovery study to determine the dye concentrations in binary solution

To verify the accuracy of the first-order derivative method, recovery studies were carried out by determining the concentrations of dyes in the binary solution [24]. To accomplish this, IB and R40 solutions were used with different concentrations of each dye, changing from 2.0 to 10.0 mg/L and keeping their concentration constant (Figs. 2(c) and (d)). Recovery percentages, error and average error were calculated using Eqs. (13), (14), and (15):

$$\text{Recovery}\left(\%\right) = \frac{C_m}{C_t} \times 100\% \qquad (13)$$

$$\text{Error}\left(\%\right) = \frac{C_m - C_t}{C_t} \times 100\% \qquad (14)$$

$$\text{Absolute average error}\left(\%\right) = \frac{\sum_{i=1}^{N}\left|\left(C_m - C_t\right)/C_t\right|}{N} \times 100 \qquad (15)$$

where C_m is the measured concentration, C_t is the theoretical concentration, and N is the data number.

Table 1 shows the recovery percentages obtained for R40 and IB in the binary mixture with the spectrophotometric method of derivatives in a range of 85.0%–100%. As can be seen, the total average error rate was 0.73% for R40 and 0.93% for IB, values lower than those reported in a similar work [24], highlighting that the method used to determine and quantify the presence of each dye in the mixture is adequate for the study system.

3.2. Influence of the initial concentration of dyes in the mixture

In order to assess the influence of the concentration of the dyes in the mixture, different amounts were taken (Supplementary Information). Fig. S1 shows that the higher the amount of the two dyes, the lower the adsorption percentage. In general, it is observed that R40 in mixture displays a more satisfactory removal compared with IB. The best adsorption percentages were presented using concentrations between 20–60 mg/L for IB and 6–24 mg/L for R40; therefore, these values will be taken into account for the evaluation of the removal of their mixture by means of a 2^4 full factorial design.

3.3. Statistical design of experiments for dye removal

3.3.1. Removal of dyes as mono-component systems

For determining the importance of the factors in the removal of individual dyes, a complete 2^3 full factorial design was implemented; the initial concentration of dye (A), adsorbent dosage (B), and contact time (C) were the selected factors. The parameters that remained constant were pH,

Table 1
Recovery percentage, error and average error of the binary mixture of IB-R40 dyes

C_t (mg/L)		C_m (mg/L)		Recovery (%)		Error (%)	
IB	R40	IB	R40	IB	R40	IB	R40
6	2	5.9	1.7	98.3	85.0	–1.7	–15.0
6	4	5.8	3.8	96.7	95.0	–3.3	–5.0
6	6	6.0	6.1	100.0	101.7	0.0	1.7
6	8	6.1	7.9	101.7	98.7	1.7	–1.3
6	10	6.3	9.7	105.0	97.0	5.0	–3.0
2	6	1.9	5.9	95.0	98.3	–5.0	–1.7
4	6	4.2	6.1	105.0	101.7	5.0	1.7
6	6	5.9	6.0	98.3	100.0	–1.7	0.0
8	6	8.1	6.1	101.3	101.7	1.3	1.7
10	6	10.2	6.1	102.0	101.7	2.0	1.7
2	2	1.8	1.7	90.0	85.0	–10.0	15.0
4	4	3.7	3.9	92.5	97.5	–7.5	–2.5
6	6	6.1	5.8	101.7	96.7	1.7	–3.3
8	8	7.8	8.0	97.5	100.0	–2.5	0.0
10	10	10.1	9.9	101.0	99.0	1.0	–1.0
				Absolute average error (%)		0.93	0.73

particle size, temperature, and agitation speed. Table 2 shows the factors and their respective levels for IB and R40.

All the experiments were conducted in triplicate to determine the experimental error, using 25 mL of dye solution at pH = 2.0, adsorbent with particle size between 0.3 and 0.5 mm at room temperature, and a stirring speed of 180 rpm.

Removal percentages of the dyes in Table 4 were calculated according to Eq. (1). In the factorial design for the individual removal of IB and R40 onto RH, it was found that the best IB removal percentages are obtained with 30 mg/L of concentration, 4 g/L of adsorbent dosage for 4 h, while for R40 a better removal is obtained with 15 mg/L of concentration, 8 g/L of adsorbent dosage, and 18 h of contact time.

3.3.2. Removal of dyes in the binary mixture

For assessing the removal of IB-R40 mixture, a 2^4 full factorial design was carried out where the selected factors were IB (A), and R40 (B) initial concentration, adsorbent dosage (C) and contact time (D). The parameters that remained fixed were pH, particle size, temperature, and stirring speed. Table 3 summarizes the factors and their respective levels for these dyes [40].

Experiments were performed in triplicate, using 12.5 mL of IB dye solution and 12.5 mL of R40 dye solution at pH = 2.0, RH with particle size between 0.3 and 0.5 mm at room temperature, and a stirring speed of 180 rpm. Removal percentages of the binary system were determined by Eqs. (9) and (10). In a similar way to what was done with individual dyes, an analysis of variance (ANOVA) (Tables S4 and S5) was carried out for the mixture, where the significance of the factors was established by regression coefficients applying the Student's *t*-test. The concentration factors of IB and R40 dyes are those that meet the 95% confidence level ($p < 0.05$). From

these data, we can determine the mixture removal through Eq. (16) as follows:

$$\%\text{Removal} = 42.8 - 7.24A - 2.16B \quad \left(R^2 = 0.9842\right) \quad (16)$$

where A and B can take the values (± 1) of IB and R40 dyes concentration, respectively. With this equation it was possible to predict the removal percentages of the selected mixture onto RH [41].

From these results, it can be established that the experimental removal percentages are similar to predicted values (Table 4), allowing to conclude that these factors (*A* and *B*) have a great influence on the removal and that the model obtained suitably represents the removal process of this dye mixture, with an average standard deviation of 3.64. In this way, the best conditions for the adsorption of IB-R40 dye mixture correspond to an initial concentration of 30 mg/L of IB, 10 mg/L of R40, 6 g/L of RH and 18 h of contact time, allowing to achieve a 64.1% removal, which is a satisfactory percentage taking into account that this is a competitive process and in addition to the low solubility that characterizes IB.

The Pareto chart for the removal of IB-R40 mixture (Fig. 3) shows that the effects exceeding the reference line correspond to IB and R40 concentration, both with a negative effect; therefore, the adsorption process is improved at the lowest concentrations of those dyes. Some effects and interactions do not exceed the effect line; therefore, they are not taken into account in the analysis due to their lower statistical significance [42].

The results above can also be observed in the main effects diagram of dye mixture removal process (Fig. S2). IB (*A*) and R40 (*B*) initial concentrations have a negative effect on removal percentage, prevailing factor *A*. The negative value of concentration coefficients of –14.94 for IB and –4.33 for R40 indicates that an increase in concentration leads to a decrease in the adsorption percentage. Thus, lower concentrations would lead to better removal. In short, the best conditions for achieving an efficient removal of the mixture were 30 mg/L of IB and 10 mg/L of R40, which were taken for the subsequent study of the equilibrium and kinetics of the dye mixture.

3.4. Adsorption isotherms of single-component and multicomponent systems

The adsorption isotherms are important to describe the interaction of dyes with the adsorbent and are useful to determine the adsorbent capacity of different materials. Table 4 shows the results of the adsorption isotherm models for IB and R40, both individually and in mixture.

3.4.1. Langmuir model

Correlation coefficients, R^2, allow determining the equilibrium model that fits the best with the experimental data. According to this criterion, results of Table 5 indicate that Langmuir model is the one that represents the best the adsorption process of R40 and IB onto RH, individually, with values of $R^2 = 0.987$ and $R^2 = 0.989$, respectively. The values of the Langmuir parameter, q_{max}, describe the saturation capacity of the adsorbent material surface in the

Table 2
Factors and levels of 2^3 full factorial design for IB and R40

Factors	IB		R40	
	Levels		Levels	
	(−1)	(+1)	(−1)	(+1)
Dye concentration (mg/L) (A)	30	50	15	20
Adsorbent dosage (g/L) (B)	4	8	4	8
Contact time (h) (C)	4	16	6	18

Table 3
Factors and levels of 2^4 full factorial design for IB-R40 mixture

Factors	Mixture	
	Levels	
	(−1)	(+1)
Adsorbent dosage (g/L)	6	10
IB dye concentration (mg/L)	30	60
R40 dye concentration (mg/L)	10	20
Contact time (h)	6	24

Table 4
2^4 full factorial design of the IB-R40 mixture removal onto RH: experimental and predicted data

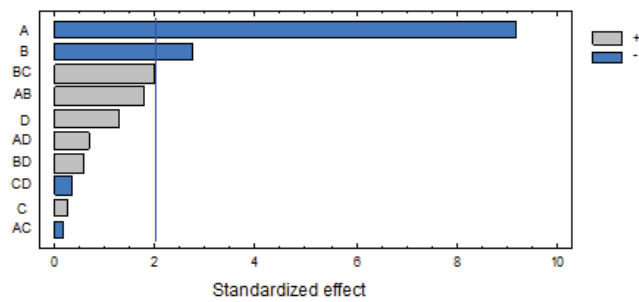| Experiment	$C_{o\,IB}$ (mg/L)	$C_{o\,R40}$ (mg/L)	DA (g/L)	TC (h)	% Experimental removal	% Predicted removal
1	60	10	6	18	36.8	37.7
2	60	20	6	18	38.9	33.4
3	60	10	10	6	40.2	37.7
4	60	10	6	6	34.3	37.7
5	30	20	6	6	44.5	47.9
6	30	20	6	18	37.7	47.9
7	30	10	6	6	56.5	52.2
8	30	10	10	18	50.7	52.2
9	30	20	10	18	45.1	47.9
10	60	10	10	18	37.4	37.7
11	60	20	10	18	39.4	33.4
12	60	20	6	6	30.0	33.4
13	30	10	6	18	64.1	52.2
14	60	20	10	6	26.2	33.4
15	30	20	10	6	37.0	47.9
16	30	10	10	6	60.4	52.2

Fig. 3. Pareto chart of the IB-R40 mixture removal percentage.

equilibrium. The maximum surface adsorption capacity for R40 and IB dyes with q_{max} of 2.74 and 6.96 mg/g, respectively, was determined at a temperature of 328 K. This clarification is important since temperature can influence this parameter. This research was carried out at four temperatures (298, 308, 318, and 328 K) and the data obtained for the most efficient removal process are shown. Additionally, it is noteworthy that the values found for q_{max} for R40 are similar to those reported in previous researches, such as the study made by Abdelwahab et al. (2005), who recorded q_{max} values between 2.42 and 4.35 mg/g for the anionic dye Direct red 23 onto RHs [43]. On the other hand, K_L is the equilibrium constant that represents adsorbate affinity for the active site of the adsorbent, as shown in Eq. (17).

$$K_L = \frac{1}{b} \qquad (17)$$

Therefore b represents the inverse of affinity [44]. Thus, from Table 5 it can be concluded that in the equilibrium, the maximum affinity between the adsorbate and the active site of the adsorbent is presented at 328 K with a K_L of 36.5 and 6.99 for IB and R40, respectively. These results are explained since the increase in temperature can favor adsorbate

Table 5
Parameters of isotherms for the single-dye systems and the binary system

Model	Parameter	Single-dye		Binary mixture	
		R40	IB	R40	IB
Langmuir	q_{max} (mg/g)	2.740	6.960	3.130	1.280
	K_L	6.990	36.50	0.095	0.286
	R^2	0.987	0.989	0.954	0.944
	η	NA	NA	1.120	1.550
Freundlich	K_F (mg/g)	0.516	0.269	0.267	0.385
	n	2.300	1.390	1.570	3.290
	R^2	0.899	0.950	0.937	0.658
Pseudo first order	k_1 (mg g^{-1} min^{-1})	2.600	10.80	0.026	0.057
	$q_{e,1}$ (mg/g)	0.960	2.530	0.574	0.252
	R^2	0.911	0.988	0.813	0.840
Pseudo second order	k_2 (mg g^{-1} min^{-1})	2.980	28.30	0.049	0.388
	$q_{e,2}$ (mg/g)	1.070	2.420	0.662	0.217
	R^2	0.970	0.989	0.908	0.850
Experimental data	q_t (mg/g)	1.090	2.480	0.900	0.170

NA, not applicable.

molecules movement and thus increase the affinity with their respective adsorbent.

3.4.2. Freundlich model

The constants of Freundlich equilibrium models K_F and n indicate the properties of the adsorbent surface and the

affinity for certain adsorbates, this allows comparing the adsorption capacities of different adsorbents. From the values of R^2 of the Freundlich isotherm, it can be concluded that this model does not offer a satisfactory adjustment since the correlation coefficients, 0.899 and 0.961, are lower than the R^2 obtained with the Langmuir model. Constants K_F and n of the Freundlich model in Eq. (3) denote the adsorption capacity and the intensity of adsorption, respectively, it should be noted that for the latter, the closer its value is to zero, the greater the surface affinity by the dye [45]. Therefore, from Table 5 it can be established that in the equilibrium, with n of 1.39 and 2.30 for IB and R40, respectively, the highest adsorption affinity at 328 K is achieved.

3.5. Multicomponent adsorption isotherms

3.5.1. Competitive extended Langmuir model

As can be seen in Table 5, an increase in the Langmuir parameter is observed, q_{max} for R40 (going from q_{max} 2.74 to 3.13 mg/g) and a decrease for IB with respect to

one-component systems at 328 K (going from q_{max} 6.96 to 1.28 mg/g). The values of q_{max} found in dye mixture suggest that there is a greater affinity between R40 molecules with the adsorbent than between IB molecules with RH [45], this fact can be explained in part to the nature of the two sulfonate groups present in R40 and their ability to generate electrostatic interactions between the adsorbate and the adsorbent, which occur mainly between those sulfonphate groups of R40 and protonated OH_2^+ groups of RH [46] compared with the low solubility of IB (see Fig. 1).

3.5.2. Modified extended Langmuir model

Regarding the evaluation of modified extended Langmuir model, it is observed from Eq. (5) that interaction factors η_1 and η_2 higher than 1.0 indicate that there is an interaction between the two dyes, being the value for IB dye higher in the mixture ($\eta_2 = 1.55$) (Figs. 4(a) and (b)), which explains the low removal of this dye in the mixture onto RH adsorbent, this finding agrees with the previous results [47].
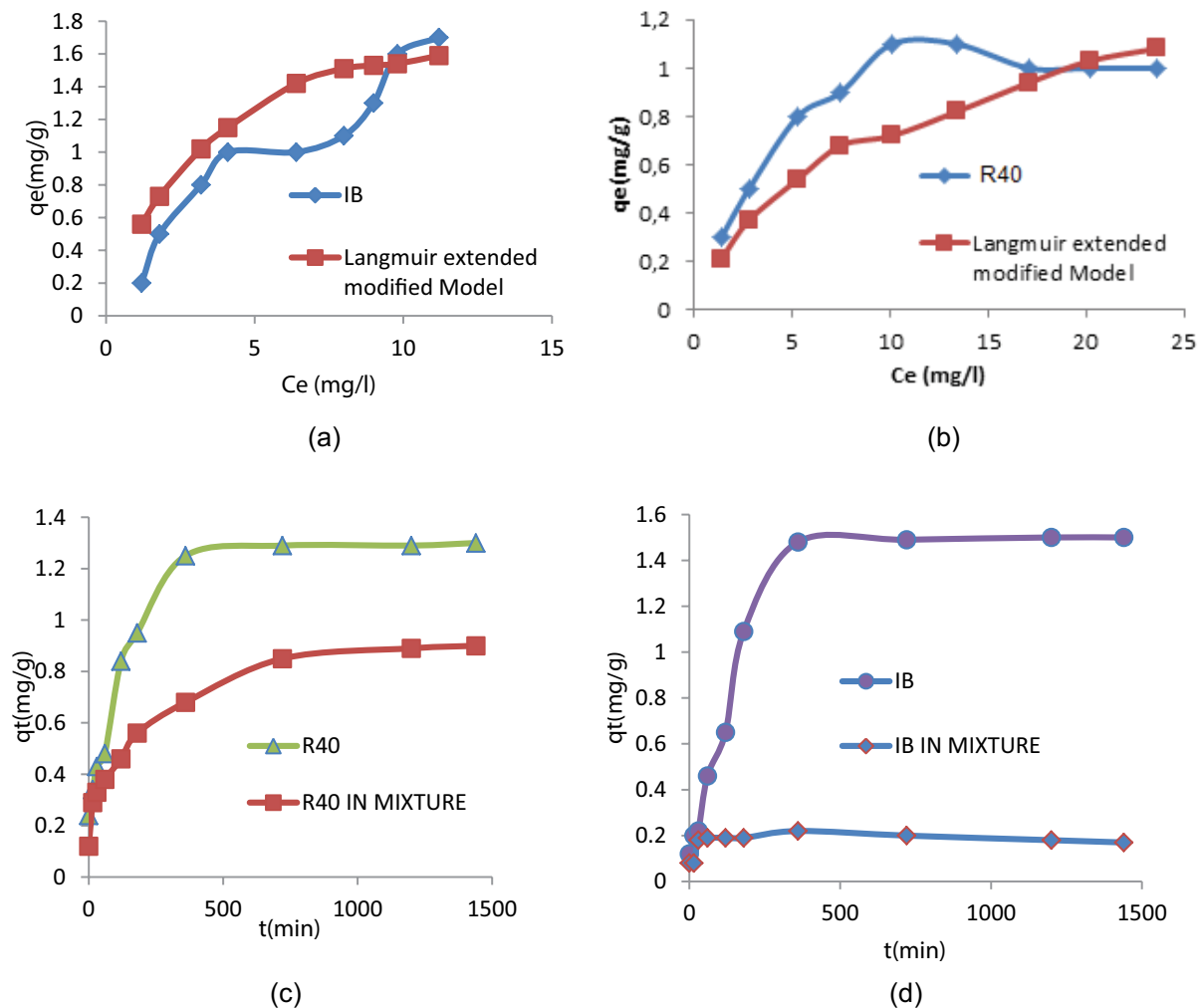

Fig. 4. (a) and (b) Experimental data of IB-R40 mixture adsorption and modified Langmuir adjustment model. (c) and (d) Comparison of adsorption kinetics of dyes as individual systems and in the dye mixture.

3.5.3. Multicomponent Freundlich model

By replacing Eqs. (7) and (8) in (6), the Freundlich constants K_F and n are obtained, which indicate adsorption capacity and adsorption intensity, respectively. When comparing multicomponent system constants with mono-component systems constants of Table 5 to 328 K, it is observed that there was no significant change in the value of n constant for R40, going from 2.30 individually to 1.57 in the mixture. While IB shows a remarkable change, going from 1.39 in mono-component system to 3.29 in the mixture, that is, an increase of more than 50% for the vat dye. A high value of n indicates that there is little affinity between the dye and RH, while n values close to zero suggest that the system surface is more heterogeneous, showing in this case the preference of RH for R40 [45].

3.5.4. Errors

For equilibrium evaluation in IB-R40 dyes mixture, unlike individual dyes, the criterion for the best fit for the model selection is given by the lowest percentage of error, for this, sum of squares (SS) and chi-square (χ^2) tests were used [33]. The following Table 6 summarizes the three models with error values.

It can be seen that the best adjustment model corresponds to modified extended Langmuir compared with the other competitive equilibrium models, since it has the lowest error values in SS and χ^2 tests. Low percentages of these tests show the similarities between the experimental data and the modified extended Langmuir model data (Table 6). Therefore, the removal of IB-R40 dyes mixture takes place through monolayers on the adsorbent surface. Figs. 3(a) and (b) plots the experimental data of the IB-R40 mixture and the modified extended Langmuir model of the binary mixture.

3.6. Analysis of kinetic models of the dye adsorption as individual systems

Adsorption kinetics of R40 and IB dyes onto RH indicates that the process satisfactorily follows the kinetic model of pseudo-second order, with a maximum correlation coefficient $R^2 = 0.970$ and 0.989 for each dye respectively at temperature of 328 K (Table 5), pointing out, therefore, that the occurrence of the process is a function of the solute initial concentration. It should be noted that these results are in agreement with those reported by researchers such as Azizian (2004), who showed that different dyes such as basic blue 169, acid blue 25 and acid red 114, offer better adjustment

to pseudo-second-order kinetics at low initial concentrations [48]. Also, it can be observed that the experimental parameter q_t at 328 K, has a great similarity with the theoretical parameter q_e value corresponding to the kinetic model of pseudo-second order (1.09 and 1.07 for R40 and 2.48 and 2.42 for IB), confirming that the adsorption of R40 and IB on RH takes place following that model. In short, the adsorption kinetics for R40 and IB dyes, evaluated individually, follows a pseudo-second-order kinetics, a model that is representative of solutions with low initial concentration of adsorbate [48].

3.7. Kinetic models of adsorption for the dye mixture

In the kinetic models analyzed at 328 K in Table 4 it is observed that for R40-IB mixture, the model with the best correlation is the pseudo-second order with $R^2 = 0.908$ and 0.850 for R40 and IB, respectively. By comparing the q_t parameter of the dyes as part of the mixture and individually, a decrease in the multicomponent system is observed, very marked for IB, ($q_t = 2.48$ mg/g and $q_t = 0.170$ mg/g) and of smaller magnitude for R40 ($q_t = 1.09$ mg/g and $q_t = 0.900$ mg/g for R40). These findings show that the removal of the dye mixture takes place competitively, as described for related systems [49] (Figs. 4(c) and (d)).

3.8. Preferential adsorption site

The separation factor was also calculated by Eq. (18) to determine which dye occupies most of the surface of RH [50]:

$$\alpha_B^A = \frac{q_A C_B}{q_b C_A} \tag{18}$$

Table 7
Separation factors of the IB-R40 dye mixture

q_{eR40} (mg/g)	C_{R40} (mg/L)	q_{eIB} (mg/g)	C_{IB} (mg/L)	α_{IB}^{R40}	α_{R40}^{IB}
0.5	4.9	0.5	6.1	1.2	0.80
0.8	7.8	0.8	9.9	1.3	0.78
1.0	10.3	0.9	13.1	1.4	0.71
1.0	13.4	1.1	16.5	1.1	0.89
1.1	14.5	1.1	19.9	1.3	0.73
1.3	17.0	1.0	23.2	1.7	0.56
1.6	19.5	1.0	26.4	2.2	0.46
1.7	21.1	0.9	29.0	2.6	0.38

Table 6
Errors for multicomponent Langmuir and Freundlich adsorption models

Model	Errors			
	SS		χ^2	
	R40 mix	IB Mix	R40 mix	IB Mix
Competitive extended Langmuir	0.268	0.208	0.675	0.603
Modified extended Langmuir	0.267	0.205	0.645	0.595
Multicomponent Freundlich	0.285	0.538	0.650	2.98

where q_A and q_B are the experimental adsorption capacities of A and B dyes, C_A and C_B are the initial concentrations of A and B dyes. If A dye is more adsorbed α_B^A separation factor is higher than 1, whereas if it is adsorbed more than B, the separation factor will be less than 1. Results show that α_{IB}^{R40} factor is between $1.2 < \alpha_{IB}^{R40} < 2.6$, and that α_{R40}^{IB} separation factor is between $0.80 > \alpha_{R40}^{IB} > 0.38$ (Table 7), which confirms the preference of the adsorbent surface for R40 over IB. These values agree with the extended Langmuir constant q_{max}, in which a higher value is obtained for R40 than for IB.

4. Conclusions

This work allowed concluding that RH by-product represents a promising adsorbent material for the removal of IB-R40 dye mixture given the satisfactory adsorption percentage reached, of the order of 64.1%, taking into account that this adsorption is a competitive process and that IB has a low solubility. Besides, the IB-R40 dyes mixture removal onto RH showed to be a competitive process with favorability for R40, with a 25% more efficient removal in comparison with IB under the best operation conditions. The higher affinity of R40 for the active sites of the adsorbent is attributed mainly to the presence of two sulfonphate groups, which promote the generation of electrostatic interactions with the active sites onto RH surface. The higher preference of RH adsorbent by the R40 dye was confirmed by the calculation of the separation factor obtaining values higher than 1.0.

The adsorption equilibrium of R40 and IB evaluated as mono-system showed better fit through the Langmuir model, since it has correlation coefficients close to 1.0, allowing to establish that removal takes place by monolayers on the adsorbent surface. For dyes binary mixture, it was found that the competitive Langmuir model adequately represents the experimental data, pointing out the competition of dyes for the active sites of the adsorbent, which was evidenced with different removal percentages for the dyes. Regarding the adsorption kinetics of R40 and IB analyzed as mono-system, a better correlation was found with pseudo-second-order kinetic model for the two dyes, with correlation coefficients close to 1.0. Concerning kinetics of the binary mixture of dyes, it was found that the kinetic model of pseudo-second-order offers the best adjustment, indicating the competition of dyes for the active sites of the adsorbent, which is verified by a decrease in the removal percentage of the dyes when they are part of the mixture.

Acknowledgments

References

[1] B. Noroozi, G.A. Sorial, Applicable models for multi-component adsorption of dyes: a review, J. Environ. Sci., 25 (2013) 419–429.

[2] K. Slater, Environmental Impact of Textiles: Production, Processes and Protection, 1st ed., Cambridge, Woodhead, 2003.

[3] K. Hunger, Industrial Dyes, Weinheim, FRG, Wiley-VCH Verlag GmbH & Co. KGaA, 2002.

[4] H.S. Jabeen, S. Ur Rahman, S. Mahmood, S. Anwer, Genotoxicity assessment of amaranth and allura red using saccharomyces cerevisiae, Bull. Environ. Contam. Toxicol., 90 (2013) 22–26.

[5] M. Honma, Evaluation of the in vivo genotoxicity of Allura Red AC (Food Red No. 40), Food Chem. Toxicol., 84 (2015) 270–275.

[6] D. Wambuguh, R.R. Chianelli, Indigo dye waste recovery from blue denim textile effluent: a by-product synergy approach, New J. Chem., 32 (2008) 2189–2194.

[7] N. Meksi, M. Ben Ticha, M. Kechida, M.F. Mhenni, Using of ecofriendly α-hydroxycarbonyls as reducing agents to replace sodium dithionite in indigo dyeing processes, J. Clean. Prod., 24 (2012) 149–158.

[8] D.I. Bernstein, Occupational asthma caused by exposure to low-molecular-weight chemicals, Immunol. Allergy Clin. North Am., 23 (2003) 221–234.

[9] N. Inomata, H. Osuna, H. Fujita, T. Ogawa, Z. Ikezawa, Multiple chemical sensitivities following intolerance to azo dye in sweets in a 5-year-old girl, Allergol. Int., 55 (2006) 203–205.

[10] D. McCann, A. Barrett, A. Cooper, D. Crumpler, L. Dalen, K. Grimshaw, E. Kitchin, K. Lok, L. Porteous, E. Prince, E. Sonuga-Barke, J. Warner, J. Stevenson, Food additives and hyperactive behaviour in 3-year-old and 8/9-year-old children in the community: a randomised, double-blinded, placebo controlled trial, Lancet, 370 (2007) 1560–1567.

[11] C. O'Neill, F.R. Hawkes, D.L. Hawkes, N.D. Lourenc, Colour in textile effluents – sources, measurement, discharge consents and simulation : a review, J. Chem. Technol. Biotechnol., 74 (1999) 1009–1018.

[12] P. Song, D.Y. Zhang, X.H. Yao, F. Feng, G.H. Wu, Preparation of a regenerated silk fibroin film and its adsorbability to azo dyes, Int. J. Biol. Macromol., 102 (2017) 1066–1072.

[13] M. Sousa, C. Miguel, I. Rodrigues, A. Parola, F. Pina, J. Seixas de Melo, M. Melo, A photochemical study on the blue dye indigo: from solution to ancient Andean textiles, Photochem. Photobiol. Sci., 7 (2008) 1353–1359.

[14] X.-H. Zhang, The study on flocculation treating wastewater from domestic animals and poultry breeding, IERI Procedia, 9 (2014) 2–7.

[15] A.-A. Peláez-Cid, A.-M. Herrera-González, M. Salazar-Villanueva, A. Bautista-Hernández, Elimination of textile dyes using activated carbons prepared from vegetable residues and their characterization, J. Environ. Manage., 181 (2016) 269–278.

[16] M. Goswami, P. Phukan, Enhanced adsorption of cationic dyes using sulfonic acid modified activated carbon, J. Environ. Chem. Eng., 5 (2017) 3508–3517.

[17] K.-W.Jung, B.H. Choi, M.-J. Hwang, J.-W.Choi, S.-H. Lee, J.-S. Chang, K.H. Ahn, Adsorptive removal of anionic azo dye from aqueous solution using activated carbon derived from extracted coffee residues, J. Clean. Prod., 166 (2017) 360–368.

[18] D.A. Giannakoudakis, G.Z. Kyzas, A. Avranas, N.K. Lazaridis, Multi-parametric adsorption effects of the reactive dye removal with commercial activated carbons, J. Mol. Liq., 213 (2016) 381–389.

[19] A. Echavarria, A., Hormaza, Flower wastes as a low-cost adsorbent for the removal of acid blue 9, DYNA, 81 (2014) 132–138.

[20] M.A.M. Salleh, D.K. Mahmoud, W.A.W.A. Karim, A. Idris, Cationic and anionic dye adsorption by agricultural solid wastes: a comprehensive review, Desalination, 280 (2011) 1–13.

[21] G. Crini, Non-conventional low-cost adsorbents for dye removal: a review, Bioresour. Technol., 97 (2006) 1061–1085.

[22] B. Jena, B.P. Das, A. Khandual, S. Sahu, L. Behera, Ecofriendly processing of textiles, Mater. Today Proc., 2 (2015) 1776–1791.

[23] V.K. Gupta, Suhas, Application of low-cost adsorbents for dye removal - A review, J. Environ. Manage., 90 (2009) 2313–2342.

[24] M. Turabik, Adsorption of basic dyes from single and binary component systems onto bentonite: simultaneous analysis of Basic Red 46 and Basic Yellow 28 by first order derivative spectro-photometric analysis method, J. Hazard. Mater., 158 (2008) 52–64.

[25] Y. Villada, A. Hormaza, Simultaneous analysis of the removal of brilliant blue and red 40 through spectrophotometric derivative, Ing. y Desarro., 33 (2015) 38–58.

[26] P. Peralta-Zamora, A. Kunz, N. Nagata, R.J. Poppi, Spectrophotometric determination of organic dye mixtures by using multivariate calibration, Talanta, 47 (1998) 77–84.

[27] A. Asfaram, M. Ghaedi, G.R. Ghezelbash, F. Pepe, Application of experimental design and derivative spectrophotometry methods in optimization and analysis of biosorption of binary mixtures of basic dyes from aqueous solutions, Ecotoxicol. Environ. Saf., 139 (2017) 219–227.

[28] J.D. Martínez, T. Pineda, J.P. López, M. Betancur, Assessment of the rice husk lean-combustion in a bubbling fluidized bed for the production of amorphous silica-rich ash, Energy, 36 (2011) 3846–3854.

[29] Dane, Censo Nacional Agropecuario Décima Entrega Resultados - 2014, Bol. Dane, Government of Colombia, Bogota, 1–43, 2015.

[30] P.C.C. Faria, J.J.M. Orfão, M.F.R. Pereira, Adsorption of anionic and cationic dyes on activated carbons with different surface chemistries, Water Res., 38 (2004) 2043–2052.

[31] A.A.B.-P. Hernández-Montoya, M.A. Pérez-Cruz, D.I. Mendoza-Castillo, M.R. Moreno-Virgen, Competitive adsorption of dyes and heavy metals on zeolitic structures, J. Environ. Manage., 116 (2013) 213–221.

[32] J. Weber, Control de la calidad del agua; Procesos fisicoquímicos, Editor. Reverté, John Wiley & Sons, New York, 1979, p. 654.

[33] K.S. Baig, H.D. Doan, J. Wu, Multicomponent isotherms for biosorption of Ni2+ and Zn2+, Desalination, 249 (2009) 429–439.

[34] S. Ziane, F. Bessaha, K. Marouf-Khelifa, A. Khelifa, Single and binary adsorption of reactive black 5 and Congo red on modified dolomite: performance and mechanism, J. Mol. Liq., 249 (2018) 1245–1253.

[35] S.K. Papageorgiou, F.K. Katsaros, E.P. Kouvelos, N.K. Kanellopoulos, Prediction of binary adsorption isotherms of Cu(2+), Cd(2+) and Pb(2+) on calcium alginate beads from single adsorption data, J. Hazard. Mater., 162 (2009) 1347–54.

[36] S. Wang, C.W. Ng, W. Wang, Q. Li, L. Li, A comparative study on the adsorption of acid and reactive dyes on multiwall carbon nanotubes in single and binary dye systems, J. Chem. Eng. Data, 57 (2012) 1563–1569.

[37] N.M. Mahmoodi, U. Sadeghi, A. Maleki, B. Hayati, F. Najafi, Synthesis of cationic polymeric adsorbent and dye removal isotherm, kinetic and thermodynamic, J. Ind. Eng. Chem., 20 (2014) 2745–2753.

[38] Y.-S. Ho, Review of second-order models for adsorption systems, J. Hazard. Mater., 136 (2006) 681–689.

[39] A.F. Halbus, Z.H. Athab, F.H. Hussein, Adsorption of disperse blue dye on iraqi date palm seeds activated carbon, Int. J. Chem. Sci., 11 (2013) 1219–1233.

[40] G. Montgomery, D. Runger, Applied Statistics and Probability for Engineers, 6th ed. New York, NY, John Wiley & Sons, 2013.

[41] A.R. Cestari, E.F.S. Vieira, A.M.G. Tavares, R.E. Bruns, The removal of the indigo carmine dye from aqueous solutions using cross-linked chitosan: evaluation of adsorption thermodynamics using a full factorial design, J. Hazard. Mater., 153 (2008) 566–574.

[42] D. Bingol, N. Tekin, M. Alkan, Brilliant Yellow dye adsorption onto sepiolite using a full factorial design, Appl. Clay Sci., 50 (2010) 315–321.

[43] O. Abdelwahab, A. El Nemr, A. El-Sikaily, A. Khaled, Use of rice husk for adsorption of direct dyes from aqueous solution: a case study of direct F. Scarlett, Egypt. J. Aquat. Res., 31 (2005) 1–11.

[44] B. Volesky, Sorption and Biosorption, BV Sorbex, Inc., Montreal, 2003.

[45] Z. Aksu, D. Akpinar, Competitive biosorption of phenol and chromium(VI) from binary mixtures onto dried anaerobic activated sludge, Biochem. Eng. J., 7 (2001) 183–193.

[46] W. Alencar, E. Acayanka, E. Lima, B. Royer, F. de Souza, J. Lameira, C. Alvesa, Application of Mangifera indica (mango) seeds as a biosorbent for removal of Victazol Orange 3R dye from aqueous solution and study of the biosorption mechanism, Chem. Eng. J., 209 (2012) 577–588.

[47] Z. Aksu, U. Açikel, E. Kabasakal, S. Tezer, Equilibrium modelling of individual and simultaneous biosorption of chromium(VI) and nickel(II) onto dried activated sludge., Water Res., 36 (2002) 3063–3073.

[48] S. Azizian, Kinetic models of sorption: a theoretical analysis, J. Colloid Interface Sci., 276 (2004) 47–52, doi: 10.1016/j.jcis.2004.03.048.

[49] S. Serrano, F. Garrido, C.G. Campbell, M.T. García-González, Competitive sorption of cadmium and lead in acid soils of Central Spain, Geoderma, 124 (2005) 91–104.

[50] H. Liu, C. Wang, J. Liu, B. Wang, H. Sun, Competitive adsorption of Cd(II), Zn(II) and Ni(II) from their binary and ternary acidic systems using tourmaline, J. Environ. Manage., 128 (2013) 727–734.
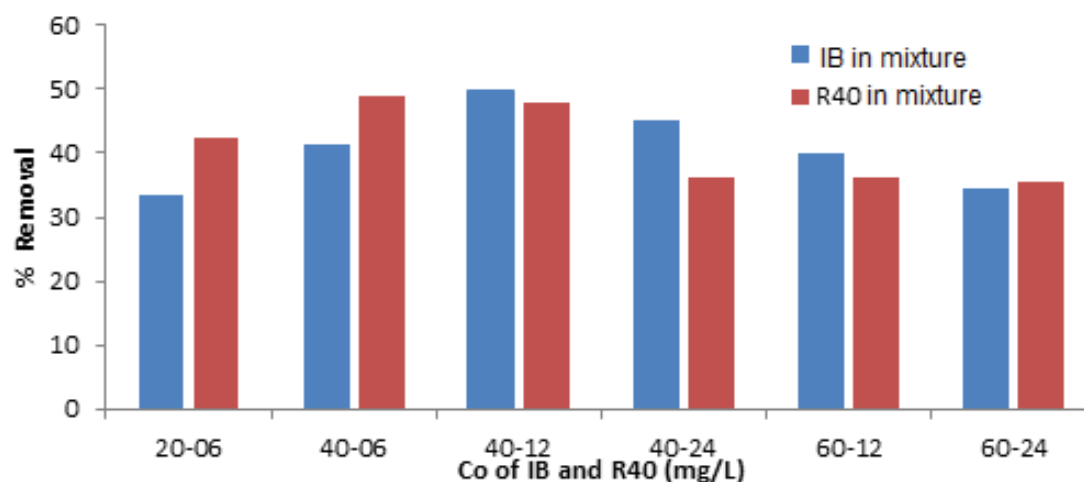
Supplementary information:

Fig. S1. Influence of the initial concentration of R40 and IB RH in the mixture, m_{CA} = 120 mg, V = 20 mL, particle size = 0.3–0.5 mm, v = 180 rpm, T = 25°C, pH = 2.0, and t = 24 h.
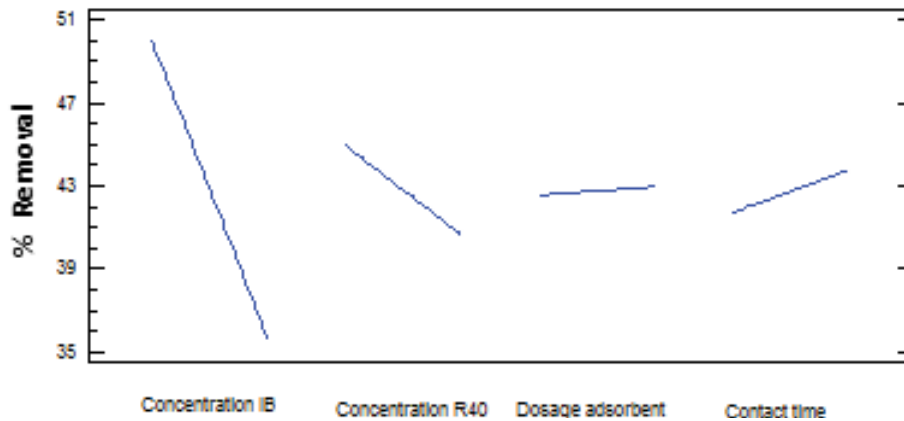
Fig. S2. Main effects on the removal percentage of IB-R40 mixture.

Table S1
Percentages of removal of IB-R40 mixture over RH at different initial concentrations

C_o IB-R40 (ppm)	IB in mixture (%)	R40 in mixture (%)	C_o IB-R40 (ppm)	IB in mixture (%)	R40 in mixture (%)
20–06	33.5	42.4	60–24	34.6	35.5
20–12	24.1	53.2	60–30	39.2	32.8
20–18	23.1	51.4	80–06	29.7	45.7
20–24	14.7	45.7	80–12	15.4	39.2
20–30	18.7	42.1	80–18	18.7	38.1
40–06	41.7	48.8	80–24	17.8	35.7
40–12	49.8	47.9	80–30	13.2	35.9
40–18	32.3	45.1	100–06	20.2	45.4
40–24	45.0	36.1	100–12	30.7	48.9
40–30	31.1	37.1	100–18	24.1	35.3
60–06	35.9	30.3	100–24	23.2	40.0
60–12	40.0	36.3	100–30	25.5	44.6
60–18	28.9	46.3			

Source: Authors.

Table S2
Estimated effects for percentage for the removal of IB-R40 mixture

Effect	Estimated	Standard error
Average	42.76	0.7882
A: IB Concentration	–14.49	1.576
B: R40 Concentration	–4.327	1.576
C: Adsorbent Dosage	0.4216	1.576
D: Contact time	2.031	1.576
AB	2.787	1.576
AC	–0.2559	1.576
AD	1.071	1.576
BC	3.172	1.576
BD	0.9566	1.576
CD	–0.5717	1.576
block	–0.6110	2.229
block	1.623	2.229

Source: Authors (STATGRAPHICS Centurion XV version 15.02.06).

Table S3
ANOVA removal of IB-R40 mixture

Source	Sum of square	Gl	Square mean	Value-p
A: IB Concentration	2,521	1	2,521	0.0000
B: R40 Concentration	224.7	1	224.7	0.0095
C: Adsorbent Dosage	2.133	1	2.133	0.7907
D: Contact time	49.51	1	49.51	0.2060
AB	93.25	1	93.25	0.0857
AC	0.7864	1	0.786	0.8719
AD	13.77	1	13.77	0.5012
BC	120.7	1	120.7	0.0519
BD	10.98	1	10.98	0.5479
CD	3.923	1	3.923	0.7190
block	16.13	2	8.065	0.7646
Total error	1,043	35	29.82	
Total (corr.)	4,101	47		

Source: Authors (STATGRAPHICS Centurion XV version 15.02.06).

Table S4
C_o, C_e, and q_e experimental of the IB-R40 mixture dyes onto RH

Mixture IB-R40 facts						
$C_{o\,R40}$ (mg/L)	$C_{e\,R40}$ (mg/L)	$C_{o\,IB}$ (mg/L)	$C_{e\,IB}$ (mg/L)	q_e R40 (mg/g)	q_e IB (mg/g)	q_e total (mg/g)
2.3	1.2	3.2	1.4	0.2	0.3	0.5
4.9	1.8	6.1	2.8	0.5	0.5	1.1
7.8	3.2	9.9	5.3	0.8	0.8	1.6
10.3	4.1	13.1	7.5	1.0	0.9	1.9
13.4	6.4	16.5	10.1	1.0	1.1	2.1
14.5	8.0	19.9	13.4	1.1	1.1	2.2
17.0	9.0	23.2	17.1	1.3	1.0	2.4
19.5	9.8	26.4	20.2	1.6	1.0	2.6
21.1	11.2	29.0	23.6	1.7	0.9	2.6

Source: Authors.

Table S5
Adjustment of the multicomponent models for the IB-R40 binary mixture onto RH

Competitive extended Langmuir model		Modified extended Langmuir Model		Freundlich multicomponent	
q_e R40 (mg/g)	q_e IB (mg/g)	q_e R40 (mg/g)	q_e IB (mg/g)	q_e R40 (mg/g)	q_e IB (mg/g)
0.59	0.22	0.56	0.21	0.58	0.35
0.76	0.38	0.73	0.37	0.65	0.61
1.03	0.55	1.02	0.54	0.87	0.93
1.14	0.67	1.15	0.68	0.98	1.22
1.39	0.70	1.42	0.72	1.34	1.41
1.46	0.79	1.51	0.82	1.49	1.73
1.46	0.89	1.53	0.94	1.52	2.11
1.45	0.97	1.54	1.03	1.54	2.43
1.49	1.01	1.59	1.08	1.65	2.69

Source: Authors.